

Investigation of the (Cu,Ga)InSe₂ thin film with different pairs of CuGa/In sputtered layers

Yu-Ting Hsu^{*a}, Kai-Feng Huang^a, Shang-I Tsai^b, Wen-How Lan^b, Ming Yueh^c, Jia-Ching Lin^d,
Kuo-Jen Chang^d, Wen-Jen Lin^d

^aDepartment of Electrophysics, National Chiao Tung University, Hsinchu 300, Taiwan, R.O.C.;
^bDepartment of Electrical Engineering, National University of Kaohsiung, Kaohsiung 811, Taiwan,
R.O.C.; ^cInstitute of Microelectronics, National Cheng Kung University, Tainan 701, Taiwan,
R.O.C.; ^dMaterials and Electro-Optics Research Division, Chung Shan Institute of Science and
Technology, Taoyuan 325, Taiwan, R.O.C.

ABSTRACT

Thin film samples of (Cu,Ga)InSe₂ (CIGS) were prepared by DC magnetron sputtering and the selenisation process onto soda lime glass substrates. All samples had the same deposition conditions, and the optimal sputtering thickness of samples with one CuGa/In pair and two CuGa/In pairs are also the same. After sample deposition, X-ray diffraction (XRD), scanning electron microscope (SEM) and Hall effect measurements were used to characterize the properties of these samples. From XRD measurement results, excepting an extra small CuSe peak existing in the samples with two CuGa/In pairs, the XRD peaks of all samples are perfectly matched with the phase diagram of CuGa_{0.3}In_{0.7}Se₂ material. It was also found that the grain sizes of the samples with one CuGa/In pair are larger than those with two CuGa/In pairs from SEM images. All these observations on samples with two CuGa/In pairs can be attributed to the fact that the less In incorporation in CIGS films, which it has been proven that the sample with low In-to-CuGa ratio has stronger CuSe peak from XRD result. Furthermore, the p-type carrier characteristics can be observed for all samples from Hall measurement results. The carrier mobility and concentration of the samples with one CuGa/In pair can be achieved as high as 15.28 cm²/Vs and as low as 1.50×10¹⁶ cm⁻³, respectively, while the carrier mobility and concentration of the ones with two CuGa/In pairs can be achieved as 6.4 cm²/Vs and 6.27×10¹⁷ cm⁻³, respectively. The results of superior electrical properties of samples with one CuGa/In pair agree well with the observations from XRD and SEM results. In the final, the optimal value of In-to-CuGa ratio during CuGa/In layers deposition in this study is 0.625.

Keywords: CIGS, high mobility, sputter, solar cell

1. INTRODUCTION

Cu(In,Ga)Se₂ (CIGS) based solar cells have received considerable attention which mainly resulted from its appropriate bandgap and its self-adjusting [1-2]. Additionally, the thickness of CIGS absorber layer is approximately 1-5μm that substantially reduces manufacturing costs of solar cells due to the lowering of materials expenses. Therefore, CIGS solar cells have been considered to be the most promising alternative photovoltaic devices. Over the past few years, Cu(In,Ga)Se₂ (CIGS)-based thin film solar cells with efficiencies exceeding 19% have been achieved by several groups [3-5]. CIGS films can be adjusted electrical property without doping. Each defect formation and each defect level of CIGS films have been calculated. Furthermore, the compositions of CIGS films influence electrical property owing to the proportion of defects [6-7]. With variation of Ga content, the band gap of CIGS films can be engineered from 1.04 eV to 1.68 eV [2]. It is necessary for band gap engineered to optimize one for high photovoltaic efficiency [3,4]. Theoretically optimal band gap of highest conversion efficiency is estimated to be around 1.4 eV. In practicality, for CIGS, it is presently limited to about 1.15 eV, due to the impact of midgap defects at higher band gaps. However, CIGS with band gap of 1.2 eV recorded champion conversion efficiency in real device. Thus, compositional study of CIGS films is required for development of high efficiency solar cell, and it is also needed for realization of multi-junction solar cells. RF sputter process is simpler for controlling and faster for depositing CIGS absorber layers than the co-evaporation process [8-10]. In this study, we report the growth and characterization of CIGS thin-films deposited on glass substrates

*alictythsu@gmail.com

by sputtering with following selenium heat treatment. The effect of thermal annealing in different ambience on the electrical property of CIGS films has also been investigated.

2. EXPERIMENTS

CIGS thin films were deposited on glass substrates (corning 1737) by sputtering technique. The glass substrates were cleaned initially by soaking in buffer oxidation etchant ($\text{NH}_4\text{F}:\text{HF}=6:1$), followed by rinsing in de-ionized water and dried in nitrogen. Then CIGS thin films were prepared by a two-stage process. First, the Copper(75%)-Gallium(25%) alloy sputtering target and Indium(99.99%) sputtering target were used to deposited CIG thin films on the glass substrates by sputtering that routinely reaches a base pressure of approximately 1×10^{-2} torr within slight flow of Ar gas. At the second stage of the process, all the samples were subsequently selenized in a partially closed chamber. Several Se pellets in a closed quartz reactor were treated by heating in the vacuum furnace. The process of selenisation was realized through two step heating profile. The first step, the samples were heated at 200°C to improve full saturation of the alloy precursor with Se, while the second step, at 550°C , was to promote chemical reactions and recrystallization of the samples. The total heating time varied up to about 20 min. Finally, electrical properties of CIGS thin films were analyzed by carrier concentration, carrier mobility through using Hall Effect measurements. The crystalline structures of the grown CIGS thin films were obtained via X-ray diffraction analysis in the range of $20-60^\circ$ with a step of 0.02° , while the surface morphology of the films was investigated using a scanning electron microscopy.

3. RESULTS AND DISCUSSIONS

For the purpose of studying the effect of the different deposition methods on the electrical properties of CIGS thin films, the various conditions of deposition were shown in Table 1. A-E samples are the CIGS thin films with one CuGa/In pair at the first stage of the process. These samples have the same thickness of CuGa layer with the following various thickness of In layer. Therefore, A-E samples have different In-to-CuGa ratio as 0.375, 0.500, 0.625, 0.750 and 0.875, respectively. It differs from other samples which are p-type CIGS thin films, the E sample which containing the most In content is n-type CIGS thin film. F-I samples are the CIGS thin films with two CuGa/In pairs at the first stage of the process. These samples have the same thickness of the first and third CuGa layers. Furthermore, these samples have the fixed thickness of the forth In layer with the various thickness of the second In layer. Consequently, F-I samples have different In-to-CuGa ratio as 0.394, 0.469, 0.550 and 0.625, respectively.

Table 1 The structure and thickness of the samples from bottom to top (I, II, III, IV) before selenising individually.

Sample	I_CuGa (nm)	II_In (nm)	III_CuGa (nm)	IV_In (nm)	In-to-CuGa ratio
A	-	-	800	300	0.375
B	-	-	800	400	0.500
C	-	-	800	500	0.625
D	-	-	800	600	0.750
E	-	-	800	700	0.875
F	400	65	400	250	0.394
G	400	125	400	250	0.469
H	400	190	400	250	0.550
I	400	250	400	250	0.625

Figure 1 shows the surface morphologies of the selenized CIGS thin films with one CuGa/In pair and various In-to-CuGa ratio at the first stage of the process. The magnification of all SEM images is 15,000. The A sample is the CIGS film containing the least In content and its In-to-CuGa ratio is 0.375. The In-to-CuGa ratio of B, C and D are 0.500, 0.625 and 0.750, respectively. It is found that the grain size of the CIGS thin film gets smaller with increasing the In content. Furthermore, it is easier to form amount of small islands at the surface with increasing the In content. Figure 2 shows the surface morphologies of the selenized CIGS thin films with two CuGa/In pairs and various In-to-CuGa ratio at the first stage of the process. The F sample is the CIGS film containing the least In content and its In-to-CuGa ratio is 0.394. The In-to-CuGa ratio of G, H and I are 0.469, 0.550 and 0.625, respectively. It is also obtained that the grain size of the CIGS thin film gets smaller with increasing the In content. Though the In-to-CuGa ratios of C and I samples are the same which is 0.625, the surface morphologies of these two samples considerably different. This phenomenon results from the various conditions of deposition at the first stage of the process. Moreover, the upper layer of the CIGS thin film with one CuGa/In pair has more In content than the one with two CuGa/In pairs. Therefore, rich In content simply leads to form the rough surface under the thermal process of selenisation.

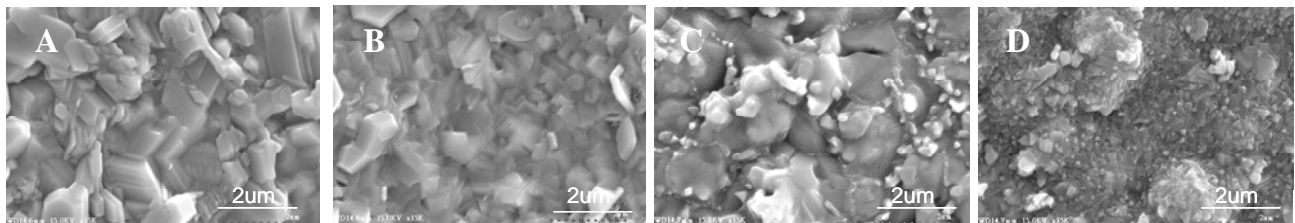


Figure 1. SEM images of the CIGS thin films deposited on glass substrates with one CuGa/In pair and the various In-to-CuGa ratio at the first stage of the process. The In-to-CuGa ratio of A, B, C, D samples are 0.375, 0.500, 0.625, 0.750.

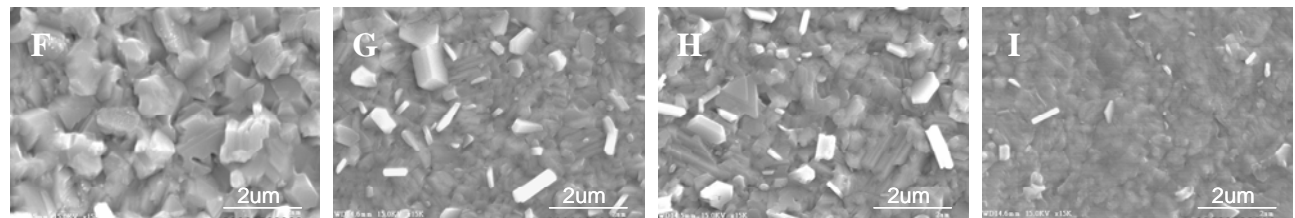


Figure 2. SEM images of the CIGS thin films deposited on glass substrates with two CuGa/In pairs and the various In-to-CuGa ratio at the first stage of the process. The In-to-CuGa ratio of F, G, H, I samples are 0.394, 0.469, 0.550, 0.625.

As shown in Figure 3, X-ray diffraction (XRD) patterns of the CIGS thin films with one CuGa/In pair indicated a typical peak at 2θ angle of 26.8° with several weak peaks at 2θ angles of 35.8° , 42.4° , 44.4° and 52.9° . Thus, it is apparent that the formation of the chalcopyrite structure of $\text{CuGa}_{0.3}\text{In}_{0.7}\text{Se}_2$ thin film is perfect. The most intense peak at 2θ angle of 28.1° illustrates the polycrystalline CIGS thin film alloy with an (112) orientation. The other prominent peaks correspond to the (211), (213)/(105), (220)/(204) and (312)/(116) phase. Additionally, it can be observed that the small amount of CuSe phase appears on A sample which containing the least In content. Furthermore, the small amount of In_6Se_7 phase appears on D sample which containing the most In content. Figure 4 shows XRD analyses of the CIGS thin films with two CuGa/In pairs. Similarly, the phases of (112), (211), (213)/(105), (220)/(204) and (312)/(116) existing in all samples are exhibited the great quality of $\text{CuGa}_{0.3}\text{In}_{0.7}\text{Se}_2$ polycrystalline thin film. The XRD patterns of all samples also indicated the presence of CuSe phase. Moreover, the intensity of CuSe phase gradually decreases with increasing In content of the CIGS thin film. Comparing with B sample of the CIGS thin film with one CuGa/In pair, the H sample with two CuGa/In pairs has higher In-to-CuGa ratio. However, it can be found that the CuSe phase appear on H sample obviously. This phenomenon results from the different stacked structure during deposition at the first stage of the process.

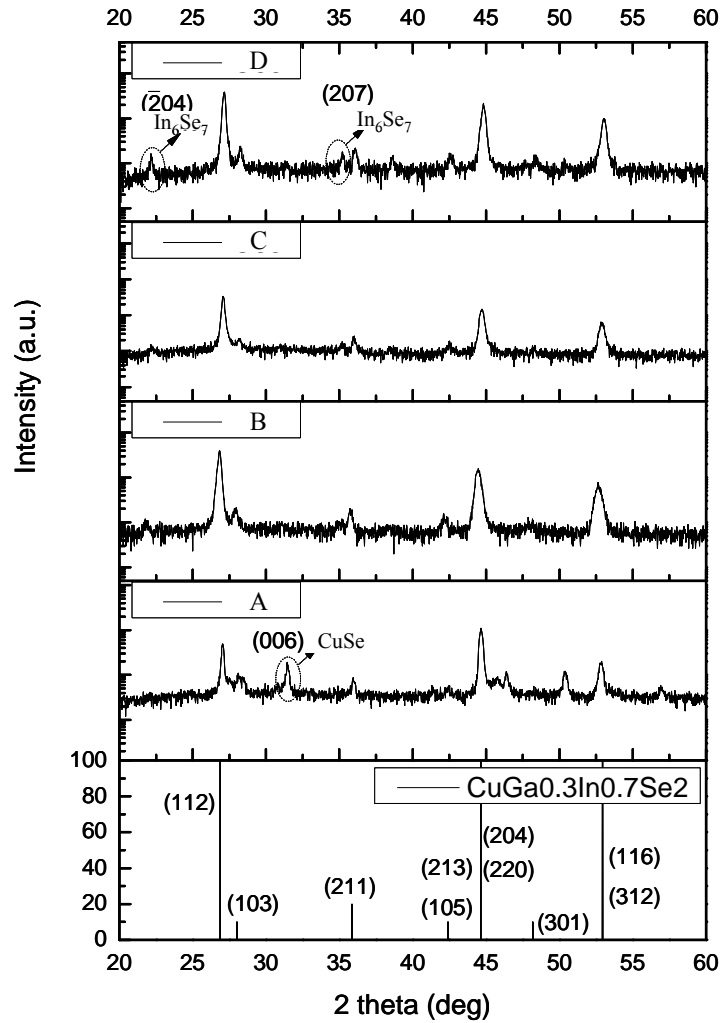


Figure 3. XRD patterns of the CIGS thin films with one CuGa/In pair and the various In-to-CuGa ratio at the first stage of the process. The In-to-CuGa ratios of A, B, C, D samples are 0.375, 0.500, 0.625, 0.750, respectively.

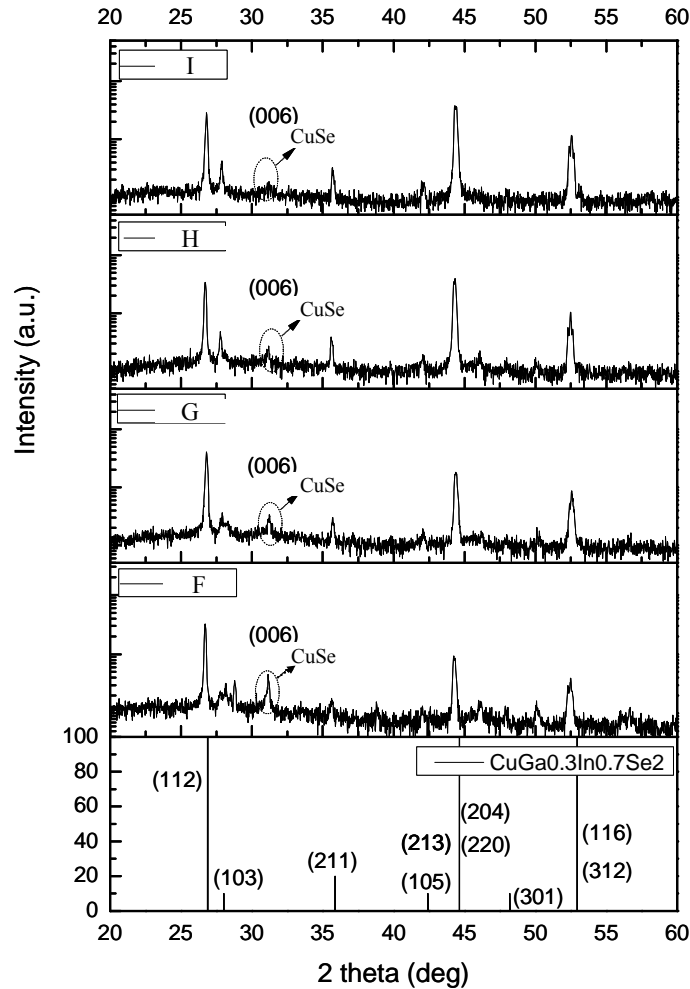


Figure 4. XRD patterns of the CIGS thin films deposited on glass substrates with two CuGa/In pairs and the various In-to-CuGa ratio at the first stage of the process. The In-to-CuGa ratio of F, G, H, I samples are 0.394, 0.469, 0.550, 0.625, respectively.

The room-temperature mobility and carrier concentration of the CIGS thin films with one CuGa/In pair, measured by Hall measurements, were shown in Figure 5. The results show that the carrier concentration gradually decreases with increasing the In-to-CuGa ratio of the CIGS thin film, while the mobility increases with raising the In-to-CuGa ratio of the CIGS thin film. Furthermore, the highest RT mobility of $15.28 \text{ cm}^2/\text{Vs}$ and lowest carrier concentration of $1.50 \times 10^{16} \text{ cm}^{-3}$ can be realized in the samples with one CuGa/In pair. It can be particularly investigated that this high room-temperature mobility of the CIGS thin films is the best so far found in the literature. Owing to the melting point of indium is low, the rich indium simply form small islands on the surface leads to the great electrical properties of the sample. Otherwise, the characteristic of E sample changes into n-type CIGS thin film on account of the CIGS films rich in In content. Figure 6 shows the carrier concentration and mobility of the CIGS thin films with two CuGa/In pairs and various In-to-CuGa ratios. It can be seen that the sample which the In-to-CuGa ratio is 0.625 has the carrier concentration as low as $6.27 \times 10^{17} \text{ cm}^{-3}$ with the mobility of $6.40 \text{ cm}^2/\text{Vs}$. Comparing to the CIGS thin films with two CuGa/In pairs, the CIGS thin films with one CuGa/In pair has the better electrical properties. The phenomenon is also well consistent with the investigations of the XRD results. The appearance of the CuSe phase in CIGS thin films will cause the lower resistivity and the higher carrier concentration. On the other hand, during the thermal process of selenisation, the rich In content simply forms In_6Se_7 phase which can increases the resistivity and decreases the carrier concentration of the CIGS thin films. This is the reason that the CIGS thin films with one CuGa/In pair have lower

carrier concentration than the films with two CuGa/In pair. Furthermore, it can be observed by SEM result that amount of small islands at the surface results from increasing the In content of the CIGS thin film. This In-rich surface can improve the mobility of CIGS thin films obviously.

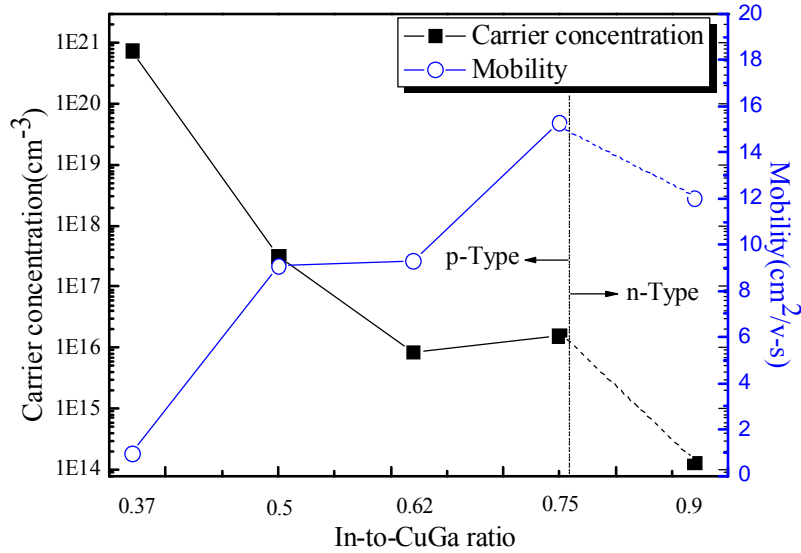


Figure 5. Room-temperature mobility and concentration of the CIGS thin films with one CuGa/In pair and the various In-to-CuGa ratio at the first stage of the process.

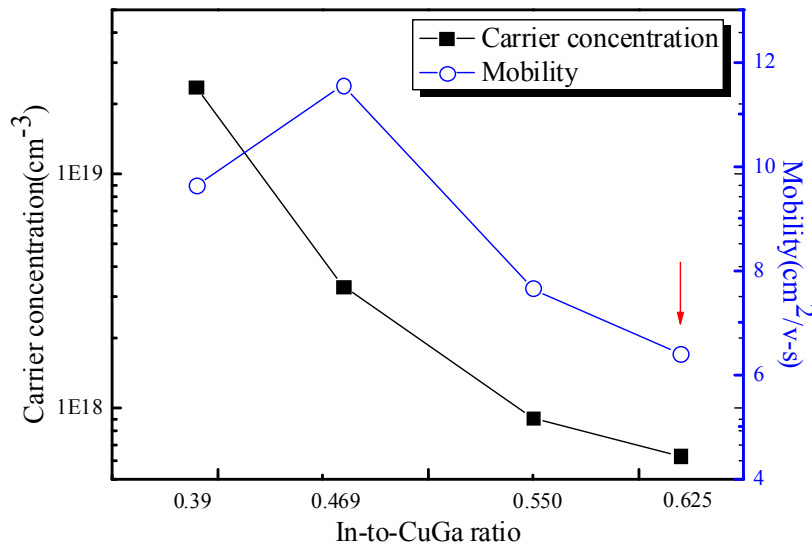


Figure 6. Room-temperature mobility and concentration of the CIGS thin films with two CuGa/In pairs and the various In-to-CuGa ratio at the first stage of the process.

4. CONCLUSIONS

High mobility CIGS thin films have been realized by DC magnetron sputtering and the selenisation process onto soda lime glass substrates. It has been studied the effect of the different deposition methods on the electrical properties of CIGS

thin films. By investigating XRD pattern, the phases of (112), (211), (213)/(105), (220)/(204) and (312)/(116) existing in all samples are exhibited the great quality of $\text{CuGa}_{0.3}\text{In}_{0.7}\text{Se}_2$ polycrystalline thin film. The highest mobility of $15.28 \text{ cm}^2/\text{Vs}$ and the lowest carrier concentration of $1.50 \times 10^{16} \text{ cm}^{-3}$ can be obtained in the samples with one CuGa/In pair. It can be particularly investigated that this high room-temperature mobility of the CIGS thin films is superior so far found in the literature. Moreover, it can be seen that the sample with two CuGa/In pairs has the carrier concentration as low as $6.27 \times 10^{17} \text{ cm}^{-3}$ with the mobility of $6.40 \text{ cm}^2/\text{Vs}$. The results are well consistent with XRD analysis mentioned above, the appearance of the CuSe phase in CIGS thin films will cause the lower resistivity and the higher carrier concentration. On the contrary, the In_6Se_7 phase increases the resistivity and decreases the carrier concentration of the CIGS thin films. It also can be observed by SEM result that the In-rich surface with amount of small islands can improve the mobility of CIGS thin films obviously. Consequently, it can be understood that the CIGS thin film with one CuGa/In pair has the excellent electrical properties.

ACKNOWLEDGMENT

This work has been supported by Materials and Electro-optics Research Division of Chung-Shan Institute of Science and Technology. Furthermore, all authors would like to acknowledge the assistance of the National Science Council, Taiwan under Contract No. NSC 98 - 2221 - E - 390 - 004 - MY2.

REFERENCES

- [1] Bekker, J., "Band-gap engineering in $\text{CuIn}(\text{Se},\text{S})_2$ absorbers for solar cells," *Sol. Energy Mater. Sol. Cells* 93, 539-543(2009)
- [2] Wei, S. H., Zhang, S. B. and Zunger, A., "Effects of Ga addition to CuInSe_2 on its electronic, structural, and defect properties," *Appl. Phys. Lett.* 72, 3199-3210 (1998)
- [3] Ramanathan, K., Contreras, M. A., Perkins, C. L., Asher, S., Hasoon, F. S., Keane, J., Young, D., Romero, M., Metzger, W., Noufi, R., Ward J. and Duda, A., "Properties of 19.2% efficiency $\text{ZnO}/\text{CdS}/\text{CuInGaSe}_2$ thin-film solar cells," *Prog. Photovolt: Res. Appl.* 11, 225-230 (2003)
- [4] Bhattacharya, R. N., Contreras, M. A., Egaas, B., Noufi, R. N., Kanevce, A. and Sites, J. R., "High efficiency thin-film $\text{CuIn}_{1-x}\text{Ga}_x\text{Se}_2$ photovoltaic cells using a $\text{Cd}_{1-x}\text{Zn}_x\text{S}$ buffer layer," *Appl. Phys. Lett.* 89, 253503-253504 (2006)
- [5] Repins, I., Contreras, M. A., Egaas, B., DeHart, C., Scharf, J., Perkins, C. L., To, B. and Noufi, R., "19.9% - efficient $\text{ZnO}/\text{CdS}/\text{CuInGaSe}_2$ solar cell with 81.2% fill factor," *Prog. Photovolt: Res. Appl.* 16, 235-239 (2008)
- [6] Lewerenz, H. J., "Development of copper indium disulfide into a solar material," *Sol. Energy Mater. Sol. Cells* 83, 395-407 (2004)
- [7] Rockett, A. and Birkmire, R. W., " CuInSe_2 for photovoltaic applications," *J. Appl. Phys.* 70, R81-R97 (1991)
- [8] Lin, Y. C., Ke, J. H., Yen, W. T., Liang, S. C., Wu, C. H. and Chiang, C. T., "Preparation and characterization of $\text{Cu}(\text{In},\text{Ga})(\text{Se},\text{S})_2$ films without selenization by co-sputtering from $\text{Cu}(\text{In},\text{Ga})\text{Se}_2$ quaternary and In_2S_3 targets," *Applied Surface Science* 257, 4278-4284 (2011)
- [9] Mahieu, S., Leroy, W. P., Aeken, K. V., Wolter, M., Colaun, J., Lucas, S., Abadias, G., Matthys, P. and Depla, D., "Sputter deposited transition metal nitrides as back electrode for CIGS solar cells," *Solar Energy* 85, 538-544 (2011)
- [10] Chen, G. S., Yang, J. C., Chan, Y. C., Yang, L. C. and Huang, W., "Another route to fabricate single-phase chalcogenides by post-selenization of Cu-In-Ga precursors sputter deposited from a single ternary target," *Sol. Energy Mater. Sol. Cells* 93, 1351-1355 (2009)